

Mev acceleration processes for heavy heliospheric ions.

Ilan Roth¹

¹*Space Sciences Laboratory, University of California, Berkeley, CA 94720, USA*

ABSTRACT

Observations of energetic ions of solar origin in the heliosphere suggest the existence of two main energization sites with different physical mechanisms: 1) impulsive mechanism on the flaring coronal magnetic field - via resonant interaction, presumably with low-frequency electromagnetic waves; 2) gradual mechanism around the propagating, interplanetary shock - by interaction with quasi-static inhomogeneous electromagnetic structure and low-frequency Alfvénic turbulence. While the coronal process enhances a subset of rare elements, the interplanetary interaction energizes most of the elements of coronal/solar wind origin. In the impulsive events, according to recent models, a significant fraction of heavy elements which reside on the active flaring flux rope is energized; the resonant interaction operates mainly on Fe and other heavy elements with high charge states. In the gradual events main energization occurs close to the Sun at low Mach numbers; significant interplanetary enhancement of energetic ion fluxes requires a narrow scale length in the propagating shock. Coupling of both processes results in the final heliospheric distribution function of the heavy elements. The enhanced energetic heavy ion population may have a profound impact on human space exploration in the interplanetary space as well as in the resulting trapped radiation in the magnetosphere.

I. INTRODUCTION

Ions of solar origin with energies of 1.0-10.0 MeV/nucleon and beyond are observed intermittently in the interplanetary space. They carry a valuable information about physical processes in the solar corona and in the heliosphere. Their abundances and isotopic states are often distinctly different from the coronal or solar wind values, which characterize the cosmic values. Some of the sites for acceleration of thermal populations to suprathermal and higher energies in the solar system include: (a) active, flaring solar corona and (b) intense, interplanetary propagating shocks. The electromagnetic shocks which emanate due to coronal relaxation processes propagate over a large fraction of the heliosphere, energizing the ambient plasma along their paths, and together with the flare-related energized populations constitute an important part of the Sun-Earth connection research theme, both being crucial to the analysis of the most intense terrestrial perturbations and risk to human activity in space.

The generally accepted paradigm makes a distinction between (a) the "gradual" events which may last for several days, being characterized by interplanetary, fast shocks carried by Coronal Mass Ejections (CMEs) with the resulting particle energization, and "impulsive" events with duration of a fraction of a day, which generate fluxes of energetic particles via wave-particle interaction on the coronal field lines. The smaller, impulsive events, involve interaction of coronal ions with waves which are correlated to the intense electron fluxes accompanying coronal release processes, and which are indirectly deduced from Bremsstrahlung radiation. The resulting resonant interaction affects several rare elements forming anomalous abundances in the energetic population; as a result one observes a dramatic abundance enhancement by factor of 10^3 - 10^5 in the isotopic ratio

of $^3\text{He}/^4\text{He}$ [Hsieh and Simpson, 1970; Mason *et al.*, 2000], and enrichment in heavier ions (mainly in Fe with high charge state of 18-22 vs 10-14 in the solar wind) by a factor up to 10 [Mason *et al.*, 1986; Reames *et al.*, 1994]. Large, gradual events indicate nonadiabatic ion trajectories in the inhomogeneous shock fields and self-generated waves with quasi-linear scattering of particles back to the propagating shock [Lee, 1983] and transport to the observing location [Reames and Ng, 1998]. Specific observations of propagating interplanetary shocks [Kennel *et al.*, 1986; Bamert *et al.*, 2004] indicate that the evolution of energetic protons follows generally the theory [Lee, 1983], with a small discrepancy in the spectrum of the resonant waves and in a more rapid decrease of the proton flux than expected from the turbulent diffusion. Some temporal and systematic variations in element abundances can be attributed to the scattering; the observed variations depend on the charge-to-mass ratio and on the generated wave spectrum, which is determined by the injected particle spectrum, i.e. shock strength and width. Besides these variations, the resulting energetic ions have relative abundances and ionization states similar to the corona [Luhn *et al.*, 1987]. Additionally, during active solar periods, after a passage of a shock, one observes energized ions with solar wind abundance as well as anomalous abundances of heavy trace ions, indicating that the heliospheric seed population may have been contaminated by previous impulsive events [Desai *et al.*, 2004]. These are the "hybrid" events which connect the coronal and heliospheric energization processes [Kallenbach, 2002].

In this paper we discuss the kinetic behavior of Fe ions interacting with electromagnetic waves on flaring coronal field and with inhomogeneous self-consistent magnetic and electric fields at the propagating shocks. This investigation may constitute a link between the global behavior of heliospheric perturbations which energize the ion populations and increase the perilous ion fluxes at Earth. We present the basic description of the interaction on coronal field lines with waves deduced from terrestrial analogy (section II), describe the shock properties (section III), investigate the intricate trajectories in the presence of the model shock (section IV), and summarize the finding in the general view of heliospheric ion acceleration (section V).

II. Energization of Trace Ions in the Solar Corona

The present coronal energization model is based on the resonant interaction with the obliquely propagating electromagnetic ion cyclotron waves (emc) [e.g., Roth and Temerin, 1997]. The frequency range of these waves is confined to below the hydrogen gyrofrequency Ω_H and above the ion-hybrid frequency. There exists an interesting analogy between physical processes on active auroral and flaring coronal field lines, as was suggested by Temerin and Roth (1992) and investigated by Miller and Vinas (1993) and Roth and Temerin (1997). Both environments consist of very low β (ratio of thermal pressure to magnetic pressure) plasmas, are dominated by two majority ion species (H and O at Earth, H and He at Sun), and are subjected to large electron fluxes due to magnetic field reconfigurations (magnetotail and coronal top, respectively). In the corona these electron fluxes are deduced from X-ray emissions, while in the aurora they can be measured *in situ* by spacecraft. Auroral observations indicate that oblique electromagnetic ion cyclotron waves, with a relatively narrow spectrum are associated with accelerated electrons which are responsible for the discrete aurora. Fisk (1978) invoked the first one stage resonant acceleration process on coronal field lines using electrostatic cyclotron waves, which required high ^4He density. Additional models of one-stage coronal acceleration include the stochastic acceleration of Fe by shear Alfvén waves (Miller and Vinas, 1993), stochastic acceleration of ^3He and ^4He by emc waves propagating parallel to the magnetic field (Petrosian and Liu, 2004; Liu *et al.*, 2004), and firehose instability due to electron temperature anisotropy (Paesold *et al.*, 2003).

The mechanism of ion acceleration is based on the gyroresonant interaction of ^3He and heavy ions. When the wave which propagates along the inhomogeneous magnetic field passes through Doppler-shifted gyrofrequency of ^3He or higher gyroharmonic of the heavier ions (mainly Fe), these ions are resonantly accelerated. The residence time in the resonance region is determined by the local gradient of the magnetic field which affects the mirror force, and by the propagation direction of the waves with respect to the magnetic field. Waves

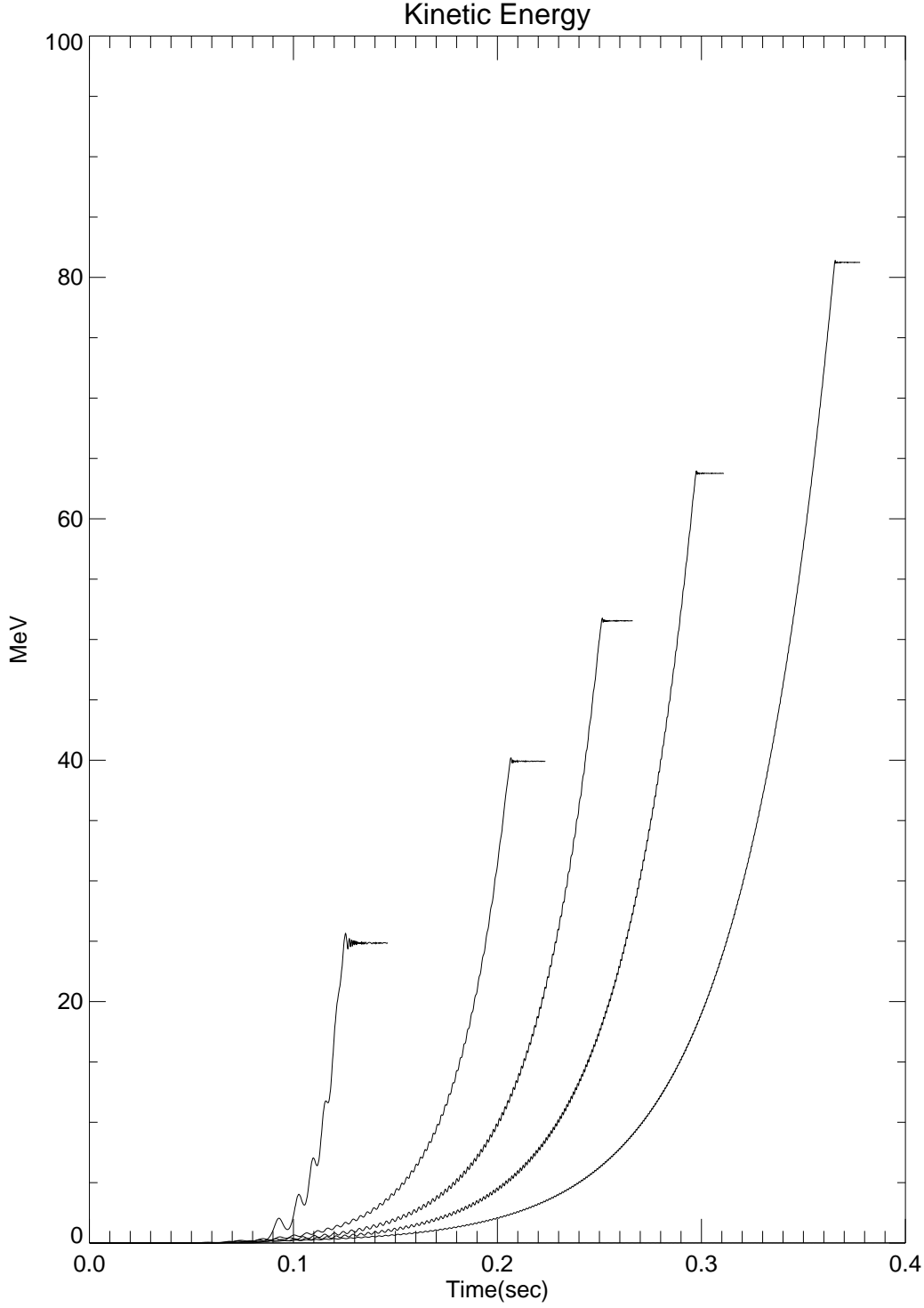


Fig. 1. Energization of Fe ions on coronal field lines by a monochromatic wave, with varying coronal charge states: $Z = 16, 18, 20, 22, 24$ (from left to right), $A=56$; $B = 500\text{G}$, $n=10^9\text{cm}^{-3}$.

propagating into stronger magnetic fields produce a parallel ion acceleration that balances the effects of the mirror force and increases this residence time, thereby enhancing the ion heating.

In the present model, an ion approaching the resonance region is subjected to two forces in the parallel direction: the mirror force due to the static inhomogeneous magnetic field, which is approximated by $B = B_o[(1 - z/L)\hat{z} + (x\hat{x} + y\hat{y})/2L]$, with a scale length L , and the oscillating wave force due to the parallel electric field and perpendicular magnetic wave field. For a monochromatic wave the electric field is described by $E = (E_x \cos \psi, E_y \sin \psi, E_z \cos \psi)$ with the phase $\psi = \int k_{\parallel}(z)dz + k_{\perp}x - \omega t$. The parallel wavenumber k_{\parallel} is related to the perpendicular wavenumber k_{\perp} and to the frequency ω via the dispersion relation which is slowly changing along the particle trajectory mainly due to the gradient in the magnetic field. In the perpendicular direction the ion takes part in gyromotion due to the external magnetic field and is subjected to the electromagnetic fields which affect its centrifugal acceleration. The electric components of the wave field are related by the dispersion relation and the magnetic components of the wave field are obtained from the Maxwell equation. The electromagnetic field amplitude required for an efficient heating is very small, since the nonlinearity in the ion trajectories needs to enhance only the residence time in the resonance region by balancing the mirror force. The normalized electric field assumed in the particle simulations satisfies $\alpha = k_{\perp}E/(\Omega B) \sim 5 \times 10^{-4}$. The parameter $\alpha \ll 1$ characterizes the strength of the wave and gives approximately the ratio of the electric field force to the magnetic field force for an ion moving at the perpendicular phase velocity of the wave near resonance. In reality one expects a broader band of waves, in contrast to monochromatic spectrum; however, since the effective energization occurs when the ion is partially trapped between the mirror and wave forces, the broader spectrum extends the heating parameter space by allowing an ion to get out of resonance with a given component of resonant wave and be trapped by another, as was shown by Temerin and Roth (1992).

Figure 1 shows the time history of Fe ions with different q/m ratios, taken from coronal distribution with varying charge states: $Z=16-24$, and $A=56$. The monochromatic wave spectrum which affects the coronal ions is adjusted accordingly to allow resonant interaction. We observe that for a given wavenumber the final energy increases with q/m or equivalently with the gyrofrequency; this energy is obtained with the ejection of the ion from the resonance domain, when the gyroradius ρ and the mirror force reach sufficiently large values and the Bessel function satisfies $J_n(k_{\perp}\rho) = 0$ (Roth and Temerin, 1997). Hence, higher charge states, which exist at the solar corona for a given temperature, may acquire higher energy, provided there exist waves which satisfy the resonant condition. This result is consistent with the observed higher charge states of Fe ions in impulsive vs gradual events. For more realistic wave spectra with a broad band spread in frequency, the spectrum of the energized ions covers the whole range between fraction of MeV to tens of MeV. These ions populate the heliosphere and may be additionally energized by the propagating shocks.

III. Properties of Propagating Shocks

Propagating interplanetary shock develops a unique inhomogeneous and highly non-linear structure. This structure consists of a relatively thin layer in which microscopic dissipation processes allow for irreversible changes in thermodynamic quantities. Electromagnetic shocks are formed due to steepening of a naturally excited wave which grows beyond the linear stage and dissipates energy in a narrow sheath. As a result, a nonlinear structure, which moves supersonically, is formed with a ramp in magnetic field, in plasma bulk velocity, density and other macroscopic quantities. The up-stream and down-stream flow regions of the shock consist of different thermodynamic states which are linked via a dissipative layer. The disparate values of the ion and electron gyroradii and the steepening and narrowing in the magnetic structure causes diversion in the trajectories of these particles. This separation of trajectories forms the necessary current which supports the magnetic field inhomogeneity, while at the same time it violates the MHD approximation, requiring kinetic description of the ensuing plasma. One way in which the frozen-in condition can be violated is via a large resistivity, which has been used by many researchers; it allows to implement successfully dissipation processes into large scale models which are being developed for space weather analysis and prediction of terrestrial perturbations (e.g. Mikic and Linker, 1994); however, this approach averages and isotropizes the behavior of plasma particles, whose trajectories depend on the detailed structure of the sheath layer, where the effect of Hall term, pressure gradients and electron inertia are often more important than the influence of resistivity. Additionally, the mesh size of the numerical global

model grossly overestimates the size of the magnetic ramp and averages over its intrinsic structure, which are crucial for the analysis of ions which form the high energy tail. The kinetic behavior of the particles which support the shock causes a small charge separation which forms a cross-shock electric field: this self-consistent field balances the magnetic field and thermal pressure forces. In an oblique shock the normal magnetic field component deflects the bulk flow, forming secondary drifts which require another component of magnetic field in the sheath region. The self-consistent electromagnetic fields, with a narrow ramp may affect profoundly a subset of particle trajectories to form an energetic tail (e.g., Balikhin and Gedalin, 1994, Gedalin *et al.*, 1995, for electrons, Zilbersher and Gedalin, 1997, for ions).

Of particular interest are the observations of the shock-related most intense fluxes of MeV ions in close proximity to the Sun, where the Mach number is low ($\sim 1 - 2$). From numerous particle simulations it is known that the turbulence for low Mach number shocks is weak, indicating that the energization is not controlled by wave reflection, as required by the diffusive shock acceleration. The main plausible mechanism for a substantial energization is related, then, to the nonadiabaticity in ion trajectories in the presence of a combined inhomogeneous electric and magnetic field.

The shock consists of a nonlinear, inhomogeneous electromagnetic structure which satisfies several conservation laws (e.g. Papadopoulos, 1985). Since almost all of the observed heliospheric shocks exhibit curvatures with very large scale lengths (many tens or hundreds of thousands of km), one may assume that locally the shock is one-dimensional, i.e. the gradients are function of only one coordinate, x . The upstream quantities are denoted by a subscript 'o'. In the case of a planar, stationary shock the magnetic field upstream of the shock region is given by $B = [B_x, 0, B_{zo}]$, downstream of the shock by $B = [B_x, 0, B_1]$, while in the shock ramp by $B = [B_x, B_y(x), B_z(x)]$. Asymptotically, the plasmas on both sides of the shock differ by density compression ratio r and rotation of the enhanced magnetic field.

From the stationary ion momentum equation and conservation of particle flux: $N(x)V(x) = N_oV_o$, one obtains the plasma flows in the shock ramp (Tidman and Krall, 1971):

$$V_x(x) = V_o - [B_y^2(x) - B_z^2(x) - B_{zo}^2]/8\pi MN_oV_o - [P(x) - P_o]/MN_oV_o$$

$$V_y(x) = [B_x/4\pi MN_oV_o] B_y(x),$$

$$V_z(x) = V_{zo} + [B_x/4\pi MN_oV_o] (B_z(x) - B_{zo}),$$

while Ohm's Law and $\nabla \times \mathbf{E} = \mathbf{0}$ give the additional ramp relations:

$$V_y(x)B_x - V_x(x)B_y(x) + (Mc/e)V_x(x)\partial_x V_z(x) + (c^2/4\pi\sigma)\partial_x B_y(x) = 0$$

$$V_z(x)B_x - V_x(x)B_z(x) - (Mc/e)V_x(x)\partial_x V_y(x) + (c^2/4\pi\sigma)\partial_x B_z(x) = -V_oB_{zo}$$

with a conductivity $\sigma = Ne/M\nu$, where ν denotes the collisional frequency. Expressing the velocities V_i as functions of B_i , assuming a specific shape for the main magnetic field component B_z and correcting it according to the last equations, allows one to obtain the ramp $B_y(x)$ component and the ambipolar cross-shock electric field, which for the chosen configuration with low β and high σ becomes

$$E_x = -V_yB_z/c + V_zB_y/c - \partial_x[(B_z^2 + B_y^2)/8\pi + P]/Ne.$$

Additionally, in the frame of the shock, there exists a motional electric field E_y , which in a stationary configuration is constant across the shock ramp. One may observe that an important contribution to B_y and to E_x is proportional to the derivative of B_z . We choose $B_z = B_{zo} 0.5 [(r+1) + (r-1)g(x/\delta)]$, with $g(x) = \tanh(x)$, or $g(x) = 0.125 [3x^5 - 10x^3 + 15x]$ in the shock region $-\delta < x < \delta$, and constant outside of the ramp, such that the ramp function and its first derivative are continuous; it describes a quantity increasing by a factor r and extending over width 2δ (Balikhin and Gedalin, 1994; Ball and Galloway, 1998). With a given pressure

profile (which can be also deduced from the energy equation) whose gradient is not of major significance for low β plasma, the spatial dependence of all the components of magnetic and electric fields are then uniquely determined. The conservation of the mass, momentum and energy flux results in a relation between the Mach number M_A , plasma β , angle of the magnetic field vs the shock surface θ , angle of the impinging upstream solar wind with respect to shock normal ϕ , and the compression ratio r .

Figure 2 shows the components of the electromagnetic field across the shock for a set of shock parameters. The magnetic field components are normalized to the upstream magnetic field, while the electric field components are normalized to the electric field resulting from the transformation between the plasma and the shock frames. It is evident that an ion which crosses the shock may be significantly influenced by an increase and rotation in the magnetic field, as well as by the cross-shock potential and the motional electric field.

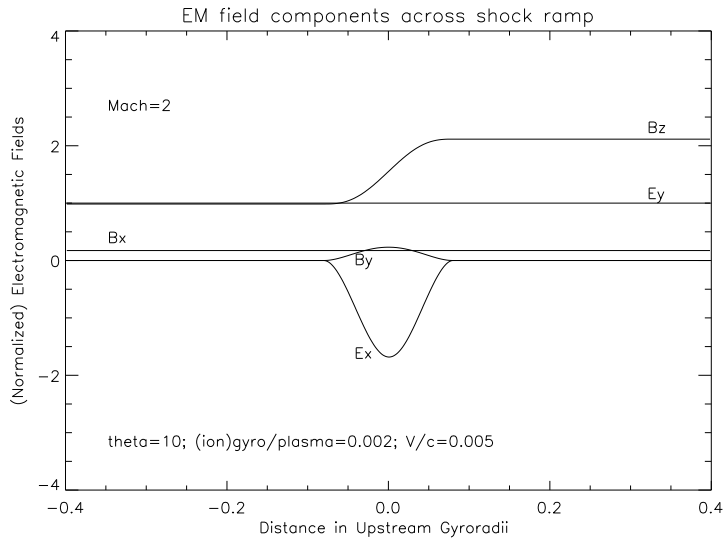


Fig. 2. Components of the electromagnetic field across the shock. Shock parameters: Mach = 2, $\beta = 0.1$, $\theta = 10.0$, $\nu = 0.01\Omega_i$. The width of the shock is one half ion skin depth: $2\delta = c/\omega_i$; ion gyro/plasma frequency ratio $\Omega_i/\omega_i = 0.002$. The gyrofrequency is given in terms of upstream bulk drift and magnetic field /gyroradius ρ : $\Omega_i = V/\rho$, $V/c = 0.005$.

IV. Trajectories of shock crossing Fe ions

During active solar periods, when a frequency of flares increases substantially, the Sun emits a significant amount of trace elements which fill a significant part of the heliosphere (e.g. Mason *et al.*, 2002). These ions, together with the thermal solar wind elements, serve as a seed population for an additional energization process due to propagating shocks. The question of energization of these trace heavy ions to high energies is of importance since Fe ion with an equivalent energy/nucleon to a hydrogen ion, is approximately 56 times more energetic, i.e. energization to 1-10 MeV/nucleon forms heavy ions with ~ 0.1 -1 GeV. These and lighter ions were observed intermittently in trapped radiation belt orbits at distances of 2-4 Earth radii after a passage of interplanetary shock (e.g. Lorentzen *et al.*, 2002), with a potentially hazardous impact on human space exploration.

In order to analyze the effect of the inhomogeneous shock structure on the trajectories of the ions we construct external electric and magnetic fields, as described in the previous section, for given parameters of the upstream plasma and Mach number. Following the results of particle-in-cell simulations various values for the shock

width were implemented: here we present results with Mach number $M_A = 2$ and shock width of tenth ion skin depth, which is plausible for an efficient acceleration. We choose a reference frame of the (propagating) shock, and follow representative ions in phase space to discern the changes in their orbits under different external conditions. For each particle we propagate in time a six-dimensional vector which describes the electron coordinates in its phase space: $\mathbf{X} = (x, y, z, v_x, v_y, v_z)$. The set of the coupled equations

$$\dot{\mathbf{X}} = \mathbf{G}(\mathbf{X})$$

where \mathbf{G} describes the prescribed, time dependent electromagnetic fields, is solved with an adaptive time step.

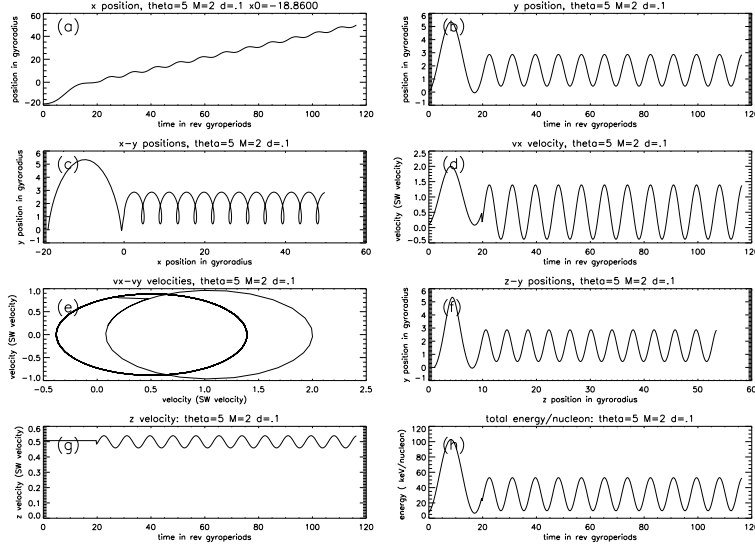


Fig. 3. Time dependence and phase space cuts in the shock frame for given Fe ion quantities: (a) $x(t)$, (b) $y(t)$, (c) y vs x , (d) $V_x(t)$, (e) V_y vs V_x , (f) z vs y , (g) $V_z(t)$, (h) total kinetic energy/nucleon vs time. Initial values: $x=-18.86$, $y=0.0$, $z=1.0$, $V_x = 0.1$, $V_y = 0.2$, $V_z = 0.5$. Shock parameters: Mach = 2, $\beta = 0.1$, $\theta = 5.0$. The width of the shock is one fifth ion skin depth: $2\delta = 0.2 c/\omega_i$; ion gyro/plasma frequency ratio $\Omega_i/\omega_i = 0.002$. The energy is measured in keV/nucleon.

The normalization used describes the time in units of the inverse upstream gyrofrequency $\Omega_o = qB_o/mc$, the velocity in the upstream average drift V_o , and distances in the upstream drift gyroradius V_o/Ω_o . The results are displayed as time series or two-dimensional projections of the phase diagram.

IVa. Shock Energization of Trace Elements.

The particles which interact with the electromagnetic inhomogeneous structure and wave turbulence while approaching and entering the shock may follow elaborate paths in phase space due to the drifts in the combined self-consistent electric and magnetic fields which form the shock. Upstream, in the shock frame, the particles gyrate around the magnetic field and drift due to the motional electric field, and as they encounter additional field components at the shock entry, the values of their energy, pitch angle and gyrophase determine the path they will follow. Therefore, the ultimate trajectory of the particle may depend not only on its energy, but also on the initial pitch angle and gyrophase. Since we are interested in low-Mach number shocks, we ignore here the turbulence excited by instabilities around the shock.

Figures 3-5 present the time sequences and phase space cross sections of Fe ions with a charge state of 20, interacting with a low-Mach shock in proximity to the Sun. In all the plots the solar wind enters the shock with

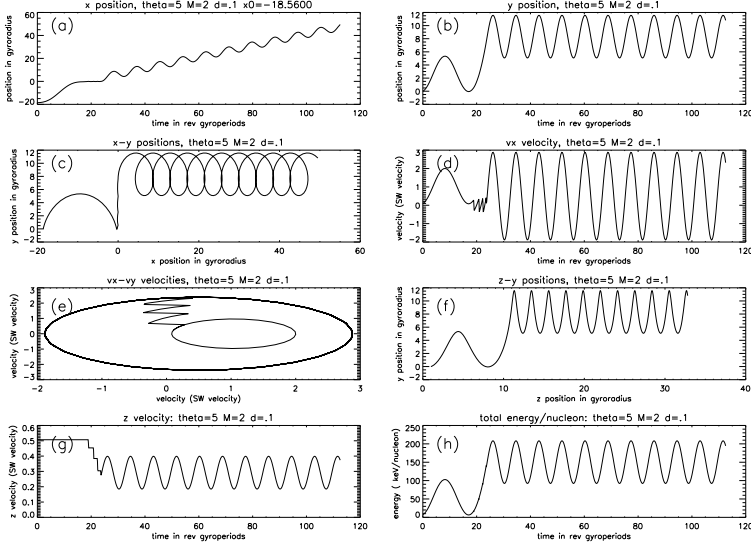


Fig. 4. Trajectory of an Fe ion, with an initial position $x=-18.58$

a velocity of 1500 km/s, for the assumed Alfvén velocity of 750 km/s, while the ratio of ion gyrofrequency to ion plasma frequency is chosen as 0.002, i.e. 10-20 times the value at 1 AU. The ions depicted on these figures differ only in their initial positions (gyrophases), with identical other initial parameters. The figures exhibit an important sensitivity to these initial conditions. Significant number of the Fe ions behave similarly to Fig. 3, where in the narrow region of shock inhomogeneity they become almost demagnetized and are decelerated due to the cross-shock electric field. Since the crossing time is much shorter than a gyroperiod, the ion does not undergo any effective drift along the shock and after crossing the shock it loses energy. Some of the ions succeed to make partial gyration during the crossing of the shock, enabling them a short drift along the shock front with a small or modest energy increase; an example is shown in Fig. 4. A small subset of Fe ions enters the shock with a small normal velocity, such that its Lorentz force is balanced by the electric force and due to the drift along the shock it acquires a significant energy (Fig. 5). During the acceleration period the ion practically stays at a given x position (frame a), oscillates with its x velocity component (frame d), traversing significant distances in y (frames b and c) and in z (frame f) directions. For a very small number of ions the balance between the trapping forces is so well satisfied that they may drift along the shock surface over very long distances and in spite of their smaller q/m ratio (vs hydrogen ions), may acquire very high energies. In the example shown the Fe ion is energized to 2 MeV/nucleon, i.e. to more than 100 MeV.

Figures 6-7 show the final distribution functions averaged over 100,000 Fe ions which enter a Mach-2 shock with skin lengths of four and eight electron scale depths, respectively. The shock propagates with a velocity of $V = 0.005 c$; the ions are initially distributed over 250 x locations, covering a distance of one gyroradius, along with 40 (10) values of v_x (v_z) in the range of 0.1 – 1.0V, i.e. in the shock frame they approximately describe a distribution with a drift of 100 keV and thermal spread of 25 keV while in the plasma frame they cover an energy range from suprathermal up to 800 keV. One observes a broad energy distribution with a tail and a cutoff: for the width of 8 skin lengths the spectrum is softer and has a cutoff at 30 MeV, while for shock width of 4 skin lengths the spectrum is harder with a cutoff around 100 MeV. Narrowing shock width allows longer shock surfing (Sagdeev, 1966; Lee *et al.*, 1996; Zank *et al.*, 1996; Lipatov *et al.*, 1997; le Roux *et al.*, 2000), resulting in a steeper spectrum and higher cutoff.

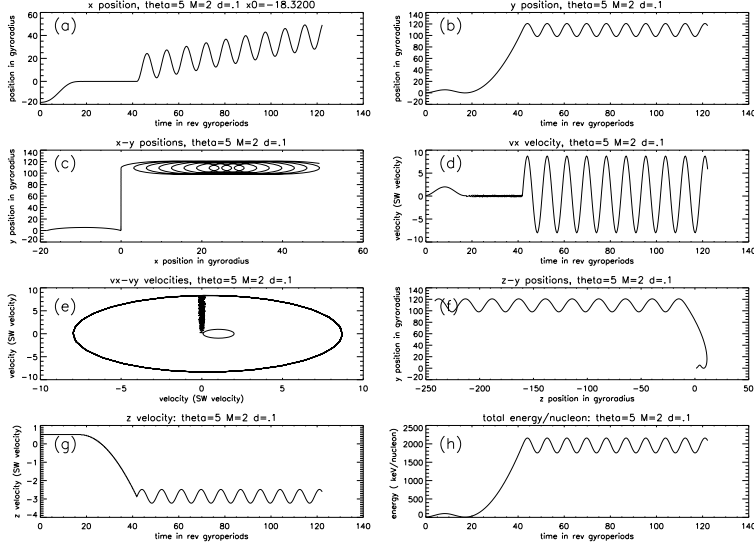


Fig. 5. Trajectory of an Fe ion, with an initial position $x=-18.32$

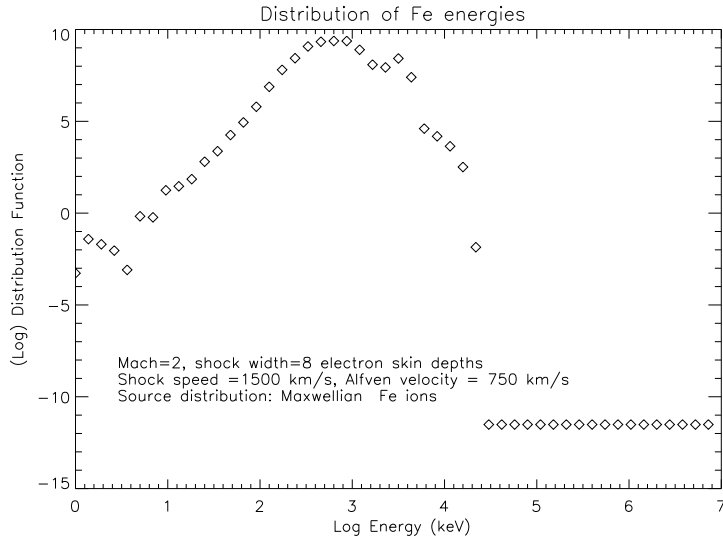


Fig. 6. Distribution function of ions averaged over the initial distribution consisting of a Maxwellian with a thermal spread of 0.5 keV. Shock width $0.2 c/\omega_i$.

V. Discussion and Summary

Coronal mass ejections, which are observed intermittently in the heliosphere, form the main *modus operandi* in which the Sun ejects minute amount of its mass, energy, and due to the magnetic field embedded in the ejected plasma, magnetic helicity. Although the amount of the ejected quantities is minuscule in comparison to the total solar content, they may have an important impact on the evolution of the solar magnetic field structure (possible accumulation of CMEs helicities over the solar cycle may contribute to the reversal in solar magnetic polarity) and on the intense perturbations of terrestrial magnetic field (magnetic storms with serious implica-

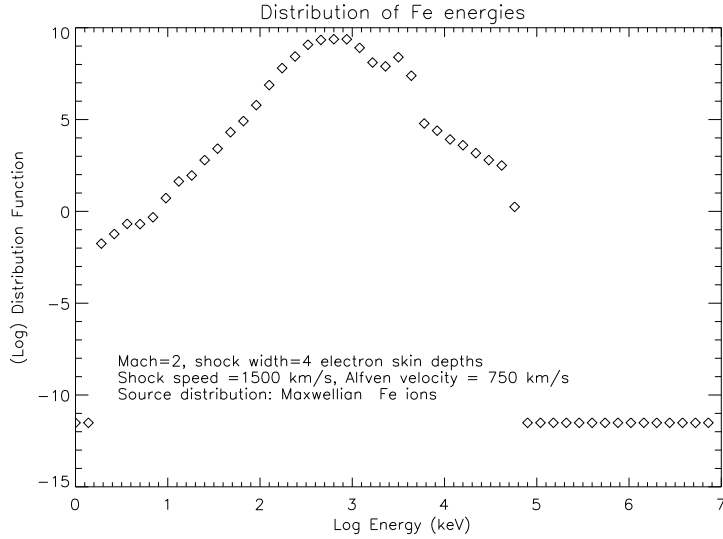


Fig. 7. Distribution function of ions averaged over the initial distribution consisting of a Maxwellian with a thermal spread of 0.5 keV. Shock width $0.1 c/\omega_i$.

tions for the functionality of human technology). The CME is often driving a shock wave ahead of it; the self-consistent interaction between the CME-driven shocks and the plowed plasma forms intense fluxes of energetic particles, while the self-consistent interaction between coronal ions and ionic waves enrich abundances which differ significantly from the solar wind/coronal values. Generally, it is a valid assumption that shock-energized particles have a very small impact on the evolution of (heliospheric) shocks, similarly to the effect of CMEs on the global evolution of the Sun. However, in the same way as the CME may be used as a tracer of phenomena occurring below the solar atmosphere, energetic particles become effectively early messengers transmitting information on processes which happen along the trajectory of the propagating shock. Since the enrichment of rare elements is correlated to an intense solar activity, it is plausible that on top of the main energization processes by the propagating shock waves, the coronal mechanism populates the heliosphere with anomalous elements which are additionally energized by the propagating shock. This may explain the coronal energization of Fe ions to tens of MeV and shock energization to hundreds of MeV. This correlation between the energization at the corona and around the propagating shocks forms the natural description of heliospheric energization and connection between both mechanisms.

An important observational aspect of ion acceleration includes the intense fluxes of energetic ions in relative proximity to the Sun, where even for the fastest propagating shocks the magnetic Mach number is relatively low (around 2-2.5). Since the turbulence at low Mach shock is generally weak, one of the best plausible shock configurations which is able to affect ion trajectories and increase substantially the energy of a subset of ions involves a narrow sheath with a significant rotation of the magnetic field and a strong cross-shock electric field. This combination of fields may "trap" some ions along the shock surface and energize them due to the motional electric field. Therefore, at the initial stage of shock propagation the turbulence level is not the crucial factor for an effective energization of the seed population. It is conjectured, therefore, that shocks which are formed at the leading edge of a CME, become the most intense accelerators of energetic particles at the low Mach values close to the Sun. At this stage of their evolution they are driven strongly by the processes which deformed the coronal field and ejected them into the interplanetary space; since they just started to plow through the background plasma, they are able to sustain a configuration of a very narrow sheath with strong magnetic field gradients, energizing the ions via shock surfing in the low Alfvén Mach numbers. At a later stage, as the shock propagates away from the sun into the interplanetary space, the sustained interaction with the plasma widens

the shock dimension, decreasing rapidly the efficiency of the shock surfing; however, the increasing Alfvén Mach number forms stronger turbulence around the shock, which enhances the diffusive shock acceleration mechanism via first order Fermi acceleration.

Several important not yet well understood topics of heliospheric acceleration include the following aspects:

1) Geometry of the coronal acceleration. Some RHESSI observations indicate that the location of the hard X rays (due to the primary flux of $>keV$ electrons), the soft X rays (due to thermal electrons on the subsequently heated coronal field lines) and the γ rays due to the energetic protons impinging on the dense coronal footpoints) do not coincide, change dynamically and at times diverge. Since the ion populations accelerated by resonant processes originate on field lines which are permeated by the suprathermal electrons, there is not necessarily a relation between the X and γ ray foot points, or equivalently, propagation of ions and electrons on flaring coronal field lines. It has been known for some time that the flux of down-going ions (inferred from the γ rays) is different from the measured ions in the interplanetary space. Tracing of energetic interplanetary ions to the corona will help to shed light on the flaring acceleration mechanism. Similarly, escape of ions from closed flaring fields is not well understood and may be due to processes similar to formation of the slow solar wind.

2) The mechanism(s) which operate on the flaring coronal field lines. Although several models attempted successfully to accelerate photospheric populations, mainly by a variety of resonantly interacting waves, the lack of in situ measurements creates a major obstacle in discerning the possible research venues. The analogy to the (observation at) aurora makes the emic as a plausible scenario, however other proposed models should be considered too. Additionally, recent observations in many impulsive events of by the WIND and ACE satellites of simultaneous energetic 3He , Fe and super-heavy elements may help in discerning the best acceleration processes. Although the question of direct emic wave excitation was not fully solved, two arguments in favor of this correlation should be made: (a) these waves are observed at the aurora together with electron fluxes, (b) electrostatic simulations indicate that due to a presence of halo electrons the turbulence spectrum is quenched at the high plasma frequencies and is shifted to low frequencies (Muschietti *et al.*, 1997).

3) The structure of the shock. The best measurements of the inhomogeneous shocks are given by magnetospheric measurements at the quasi-stationary bow shock, which indicate the rotation of the magnetic field and the existence of the cross-shock potential. Many particle simulations indicate the possibility of dynamical narrowing of shocks with a subsequent weakening and reformation over time scale of ion gyrofrequency. Although the shocks which emanate from the corona satisfy similar boundary conditions to the geophysical shock, their formation due to violent coronal magnetic reconfiguration, fast buoyancy-related acceleration and high propagation speed may suggest that they may carry a substantially steeper electromagnetic fields. Similarly, the structure depends (to some extent) on the equation of state or on the (nonadiabatic) processes which dissipate energy and sustain the shock. Future observations will shed light on these aspects.

In summary, the inhomogeneous field of the flaring corona and of the propagating shock identifies a subset of elements and ions, which acquire energy of $\sim 1-100$ MeV/nucleon through interaction with waves and combined drift in the electromagnetic fields, respectively. The excitation of electromagnetic waves below H gyrofrequency and the inhomogeneity of the magnetic field determines the coronal acceleration. The narrowness of the magnetic ramp is the crucial factor which determines the effective acceleration, decreasing the need for turbulence in the low-Mach number shocks. The shock serves also as an additional accelerator for ions which were energized on the coronal field lines; it applies particularly to the heavy ions (Fe, Mg) which may acquire an energy of a fraction of GeV.

ACKNOWLEDGEMENTS

The work was supported, in part, by NASA grants FDNAG5-11733 and FDNAG5-11944 and by NSF contract BU-GC177029NGA. The author thanks the referee for the constructive remarks about the manuscript.

REFERENCES

- Balikhin, M., and M. Gedalin, *Geophys. Res. Lett.*, **21**, 841, 1994.
- Ball, L., and D. Galloway, *Jour. Geophys. Res.*, **103**, 17455, 1998.
- Bamert, K., R. Kallenbach, N.F. Ness, Smith, C.W. Terasawa, T. Hilchenbach, R.F. Wimmer-Schweingruber and B. Klecker, *Astrophys. J.*, **601**, L991, 2004.
- Desai, M.I., Mason, G.M., Wiedenbeck, M.E., Cohen, C.M.S., Mazur, J.E., Dwyer, J.R., Gold, R.E., Krimigis, S.M., Hu, Q., Smith, S.W., and Skoug, R.M, *Astrophys. J.*, **611**, 1156, 2004.
- Fisk, L.A., *Astrophys. J.*, **224**, 1048, 1978.
- Hsieh, K.C. and J.A. Simpson, *Astrophys. J. (Lett.)*, **162**, L191, 1970.
- Gedalin, M., K. Gedalin, M. Balikhin and V. Krasnosselskikh, *Jour. Geophys. Res.*, **100**, 9481, 1995.
- Kallenbach, R., *Adv. Space Res.*, **30**, 91, 2002.
- Kennel C.F., F.V. Coroniti, F.L. Scarf, W.A. Livesey, C.T Russell and E.J. Smith, *Jour. Geophys. Res.*, **91**, 11917, 1986.
- Lee, M, *Jour. Geophys. Res.*, **88**, 6109, 1983.
- Lee, M.A., V.D. Shapiro and R.Z. Sagdeev, *Jour. Geophys. Res.*, **101**, 4777, 1996.
- le Roux, J.A., H. Fichtner and G.P. Zank, *Jour. Geophys. Res.*, **105**, 12577, 2000.
- Lorentzen, K.R., J.E. Mazur, M.D. Looper, J.F. Fennell and J.B. Blake, *Jour. Geophys. Res.*, **107**, 1231, 2002.
- Liu S., V. Petrosian and G.M. Mason, *Astrophys. J.*, **613**, L81, 2004.
- Lipatov, A.S., G.P. Zank and H.L. Pauls, *Jour. Geophys. Res.*, **103**, 29679, 1998.
- Luhn, A., B. Klecker, D. Hovestadt and E. Möbius, *Astrophys. J.*, **317**, L951, 1987.
- Mason, G.M., D.V. Reames, B. Klecker, D. Hovestadt and T.T. von Rosenvinge, *Astrophys. J.*, **303**, 849, 1986.
- Mason, G.M., J.R. Dwyer and J.E. Mazur, *Astrophys. J. (Lett.)*, **545**, L157, 2000.
- Mason, G.M., J.E. Mazur and J.R. Dwyer, *Astrophys. J. (Lett.)*, **565**, L51, 2002.
- Mikic, Z., and J.A. Linker, *Astrophys. J.*, **430**, 898, 1994.
- Miller, J.A. and A.F. Vinas, *Astrophys. J.*, **412**, 386, 1993.
- Muschietti L., I. Roth and G. Delory, *Jour. Geophys. Res.*, **102**, 27217, 1997.
- Petrosian, V. and S. Liu, *Astrophys. J.*, **610**, 550, 2004.
- Paesold, G., R. Kallenbach and A.O. Benz, *Astrophys. J.*, **582**, 495, 2003.
- Papadopoulos, D., in *Collisional shocks in the Heliosphere*, AGU, ed. Tsurutani and Stone, 1985.
- Reames, D.V., J.P. Meyer and T.T. von Rosenvinge, *Astrophys. J. Supp.*, **90**, 649, 1994.
- Reames, D.V. and C.K. Ng, *Astrophys. J.*, **504**, 1002, 1998.
- Roth, I. and M.A. Temerin, *Astrophys. J.*, **477**, 940, 1997.
- Sagdeev R.Z. Review of Plasma Physics, **4**, 23, 1986.
- Temerin, M., and I. Roth, *Astrophys. J. (Lett.)*, **391**, L105, 1992.
- Tidman, D.A. and N.A. Krall, *Shock Waves in Collisionless Plasmas*, Wiley Interscience, NY, 1971.
- Zank, G.P., H.L. Pauls, I.H. Cairns, and G.M. Webb, *Jour. Geophys. Res.*, **101**, 457, 1996.
- Zilbersher, D., and M. Gedalin, *Planet. Space. Sci.*, **45**, 693, 1997.